Frost Heave and Ice Lenses Formation in Freezing Soils

Leonid Bronfenbrener*

Ben-Gurion University of the Negev, P. O. Box 653, Beer Sheva, 84105, Israel

Abstract: A generalized model for secondary frost heave in freezing fine-grained soils is presented and discussed. The cryostatic suction effect, which increases upward water permeation, ice-lens growth during freezing, and, as a consequence, the increase of soil heave, is considered to be the main mechanism of moisture transfer. We recognize the need to determine the distribution of the moisture within the frozen fringe by approximation of the experimental data for the equilibrium unfrozen water content. This distribution is the result of the complicated interaction between water, ice and the mineral skeleton during the freezing process. The generalization of the Clapeyron relation, which is used in the studies of other authors, estimates only the drop in initial freezing temperature and does not define the connection with the external temperature gradient ∇T, which is responsible for the frost heave process. This very important aspect is discussed in detail in the introduction to our paper. We take also into account the ratio $Pe/Ste \neq 1$ (where $Pe \ll 1$). This approach allows us to obtain a more general solution. The criterion of the ice lenses formation in fine-grained soils and the model for calculation of the lenses' thickness and spacing are derived. The dynamics of the lenses formation in histogram form is presented and discussed. The theoretical results obtained from the solution for fine-grained soils are compared in good agreement with experimental investigations. The model presented predicts the frost heave and ice lenses formation in freezing soils with reasonable accuracy, satisfactorily reflects observed phenomena, and thus can be suitable for engineering practice.

Keywords: Frost heave, Frozen fringe, Ice lenses formation, Equilibrium unfrozen water content, Frozen and unfrozen soil, Overburden pressure.

1. INTRODUCTION

The effects of the harsh climate found in regions such as Canada, The United States and North-East Asia on civil engineering structures cannot be neglected by designers and contractors. For example, in the Province of Quebec, with freezing indices ranging from 800 to over 2000 degree-days, frost penetrates to depths greater than 1.5m and frost action mainly develops in frost-susceptible soils, leading to ice lens formation, surface heave, and eventual distress of structures [1]. In regions with even colder climates such as Siberia in The Russian Federation, freezing indices of 4000 to 6000 degree-days are found with frost penetration to depths greater than 2.5m [2]. Nevertheless, it should be noted that frost action in the freezing soils is often ignored. When granular soils, such as sand, are subjected to freezing, the moisture in the soil undergoes phase change, forming what is referred to as pore ice. This freezing process is often called freezing *'in situ'*. The presence of finer particles in these soils can modify their frost susceptibility. A slow-moving freezing front may cause unfrozen moisture movement toward the freezing front, and induce an accumulation of ice [3-6]. In this case, the soil promotes the formation of ice lenses during the freezing processes, leading to *frost heaving*, i.e. the upwards displacement of the soil surface. Understanding the phenomenon and the development of predictive tools will allow for the anticipation of the adverse consequences of frost heaving on structures and preventing these consequences at the design stage.

The scientific investigation of frost heave goes back to the 1920s. Studies of soil freezing were performed by Taber [7, 8]. They showed that the increase in volume is not only due to the different densities of water and ice, but mainly due to a water migration process from the unfrozen part of the soil towards the freezing front and demonstrated the phenomenon of frost heave. Other early contributions to frost heave research are those of Beskow [9]. He noted the similarity between unfrozen water content during soil freezing and residual water content encountered during soil drying. This led some (e.g. [10,11]) to suggest that water transport during frost heave is akin to the capillary rise of water into a dry porous medium, driven by surface tension at the interfaces between ice and pore water.

It is interesting that the capillary theory of water flow and frost heaving based on the Laplace surface tension equation both became popular in the 1960's and 1970's. The simplicity of the capillary theory was appealing, but experimental tests did not confirm its validity: heaving pressures during freezing tests were found to be significantly larger than those predicted by the theory. In addition, there was also evidence that ice lenses can form within frozen soil at some distance

*Address correspondence to this author at the Ben-Gurion University of the Negev, P. O. Box 653, Beer Sheva, 84105, Israel; Tel: +972-50-8504696; Fax: +972-8-6889531; E-mail: lebr@012.net.il

from the freezing front, which could not be explained by the capillary theory. Moreover, it is known from experimental [3, 4, 12-15] and theoretical [5, 6, 16, 17] studies of freezing processes that the front of macroscopic ice formation lags significantly behind the boundary of incipient freezing. Due to the physical incompetence of the capillary mechanism, hypotheses about the existence of capillary forces in freezing soils have not been further developed.

It is known that in soils such as silt, clay and loam, only a portion of the water (pore water) will freeze at the freezing point, and some liquid water will remain at sub-freezing temperatures. This equilibrium unfrozen moisture content depends on the specific surface of the soil [18-20]. The lowering of the water freezing temperature in porous media is a result of the very complicated energetic interactions of the active mineral surface with free and bound water. In this respect the equilibrium unfrozen water content distribution, which can be determined experimentally, reflects the total effect of these interactions during the crystallization process and ice formation [3,4,20-24].

There is a significant amount of literature that considers the mathematical analysis of, so called, primary frost heave models without frozen fringe formation (see e.g. review by Fasano and Primicerio [25]). Nevertheless, in general, these models do not consider ice lens formation or any heave of the soil surface. However, as experimental investigations show [3, 5, 12, etc.], the macroscopic ice formation (ice lenses) lags significantly behind the boundary of incipient freezing.

An approach for the prediction of segregation potential using the frost heave response was carried out by Konrad [1]. This approach was based on frost heave characteristics of fine-grained soils.

It is well known in practice, that the frost heave mechanics can be regarded as a problem of impeded penetration of a layered medium by an ice-water interface that exists in the frozen soil at the front of macroscopic ice formation. In this respect a great deal of attention is paid on the studies and models of O’Neill [26] and O’Neill and Miller [27]. A mathematical description of this model is often called the *rigid ice model* for secondary frost heave. According to this model, the pore ice and ice lenses are treated as one body and heave rate is related to the ice velocity, which, in this case, will be independent of spatial coordinates and only a function of time, i.e. $\mathbf{v}_s = \mathbf{v}_i(t)$.

The secondary frost heave theory based on a *thermal regelation mechanism* was first modeled by Gilpin [28] and discussed in the context of interfacial premelting by Worster & Wettlaufer [29]. In accordance with Gilpin's concept, the conditions for frost heave rate can be written as $\mathbf{v}_i - \mathbf{v}_s = -\lambda \nabla T$, where λ is an empirical constant.

In the work of Fowler & Krantz [30] the generalized secondary frost heave model is presented. Although the authors' comment that their “Generalized model can predict the frost heave behavior of different soils and agree with the results of qualitative observations”, their study suffers from a common fault of a lack of qualitative comparison with the calculations of other authors and experimental verification.

Another important aspect of the problem should be noted. In the studies of O'Neill and Miller [27], Fowler and Noon [31], Fowler & Krantz [30] and Noon [32] it is assumed that the distribution of temperature in the frozen fringe is given by a generalization of the Clapeyron relation, accounting for the effect of both pore pressure and capillary suction at the freezing temperature. However, it is well known that the Clapeyron relation estimates the reduction ΔT of the *initial freezing temperature* of water in the porous media and does not characterize the temperature distribution in the frozen fringe. As was shown in study by L. Bronfenbrener and R. Bronfenbrener [33], the temperatures, calculated according to the Clapeyron relation for a wide range of moisture and pressure, are around initial freezing temperature of water. In particular, it follows from the calculations that $\Delta T = 0.4°C$. We also note, as the experimental investigations show [3, 4, 21, 23, 24, 34], the *initial temperature of crystallization* (phase transition) in fine-grained soils such as silty loam, silt and clay varies from -0.3 to -0.5^{o}C.

In general the frozen fringe – freezing zone, where crystallization and unfrozen water migration take place simultaneously, is defined from the solution of the boundary movement problem (see for example [25, 35-37]). The moisture in this zone is characterized by the redistribution of the unfrozen water content in a relatively wide temperature interval. From experimental investigations on the equilibrium unfrozen water content, this interval is approximately -0.3 to -14 ^{o}C. In this context we note (for example) that the moisture at the front of lens formation W_l in the study of Fowler & Krantz [30, p.1666] is equal to 0.2. From experimental distributions (see Figure **1A**) this moisture conforms (approximately) to the temperature -1.4 ^{o}C and -6.6 ^{o}C for the silt and clay, respectively, and it is not in agreement with the temperature distribution based on the Clapeyron relation.

In contrast to model of Fowler & Krantz [30] in our opinion the utilization of an equilibrium unfrozen water content for finding the experimental moisture distribution allows us to obtain the gradient of the moisture at the front of most recent ice lens formation and, as a consequence, to estimate the water permeation flux. This distribution characterizes a total result of the very complicated energetic interaction of the active mineral surface with free and bound water and ice. *It is very important to recognize that the distribution of the equilibrium unfrozen water content is controlled by the external (given) gradient* ∇T *and in this manner bound up with it.* On the contrary, the generalization of the Clapeyron relation, which is used in the work cited above, only estimates the drop in initial freezing temperature and does not define the connection with the external temperature gradient ∇T, which is responsible for the frost heave process. This very important aspect is discussed below.

In this respect the analysis and treatment of experimental data in dimensionless variables carried out by Bronfenbrener and Korin [6, 23] leads to the following approximation function, which is in close agreement with experimental distributions (Figure **1B**):

$$\omega_{eq}(\theta) = \frac{1+\theta}{1-a_0\theta}, \tag{1.1}$$

in which

$$\theta = \left(T - T_f\right)/\left(T_f - T_s\right), \tag{1.2}$$

$$\omega_{eq} = \left(W_{eq} - W_{\min}\right)/\left(W_0 - W_{\min}\right). \tag{1.3}$$

In these last expressions, θ and $\omega_{eq}(\theta)$ are the dimensionless temperature and equilibrium unfrozen water content; T_f and T_s are initial phase transition temperature at the freezing front and at the soil surface. They define the temperature gradient in the freezing zone; $W_{\min} = W_{eq}(T_s)$ and a_0 are the moisture at the cold (top) boundary of the soil (or sample), and the constant parameter for approximation of $\omega_{eq}(\theta)$ related to the type of the soil, respectively.

In the present study, for the unfrozen water content we used the dimensionless approximation (1.1) of the experimental data, and verified the model by comparison with experimental results for the freezing process in clay, silt and sandy soils (Figure **1B**). We also give the solution in dimensionless form, including the criteria which characterize the relative effect of the convective and phase transition components on frost heave and freezing front propagation.

Thus, in this paper, based on the generalized model of secondary frost heave during the soil freezing process [33], we present the criterion of the ice lenses formation. In this respect the model for calculation of the lenses thickness and spacing are derived. The histogram of the lenses formation dynamics with appropriate values of the frost heave is presented and discussed. The results obtained in this study are in close agreement with those from experimental investigations.

2. PHYSICAL BACKGROUND AND STATEMENT OF THE PROBLEM

In this section we present a description of the physical background, geometry and equations for frost heave during the soil freezing process. The initial,

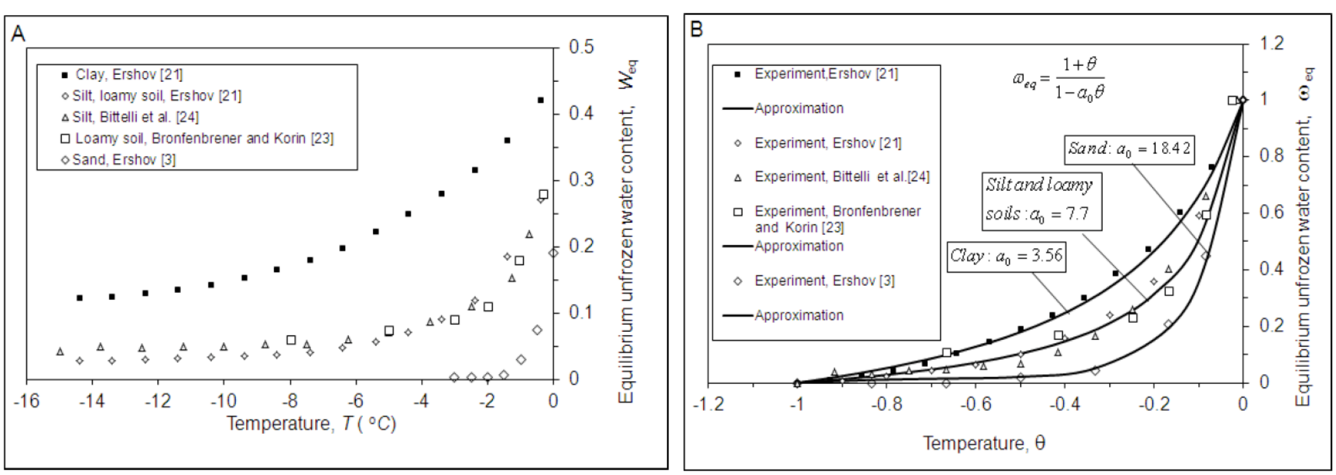

Figure 1: Equilibrium unfrozen water content: **A** – experimental data of Ershov [3, 21], Bittelli *et al.* [24], Bronfenbrener and Korin [23]; **B** – dimensionless approximation.

boundary, and supplementary conditions and relations for the solution are presented. It is also derived and discuss criterion of the ice lenses formation.

2.1. Energy and Mass Conservation Equations

We consider the process of soil freezing from the top down. The coordinate z is positive and above its origin that is fixed at some point in the unfrozen part of the soil.

We will also assume that the unfrozen part of the soil is kept saturated with water at all times. Initially (at $t=0$) the homogeneous porous medium has a uniform moisture distribution $W=W_0$ and a temperature T_0 that is higher than T_f, which is defined as the initial phase-transition temperature related to the water content, $W_f=W_0$. At time $t>0$ the top boundary of the system (heaved soil surface) $z_s(t)$ is held at the constant temperature T_s, which is lower than the initial phase-transition temperature, and the whole domain is divided into three zones: (1) the frozen zone $z_l(t)<z<z_s(t)$, which is defined as the region between the cooling boundary $z_s(t)$ and the bottom of the most recently formed ice lens position – $z_l(t)$; (2) the frozen fringe (freezing zone) $z_f(t)<z<z_l(t)$ where $z_f(t)$ is the freezing front position coordinate; and (3) the unfrozen zone $z<z_f(t)$. We also define a basal plane at $z_b \geq 0$, below the maximum depth of freezing z_f, at which the temperature and water pressure are assumed to be known (Figure **2**).

We note that for the prediction of the laboratory experiment or treatment of the experimental data the z_b coordinate can be chosen as the origin of the coordinate system, i.e. $z_b=0$. In the frozen zone the temperature varies within the interval $T_s \leq T \leq T_l$, where T_l is the temperature at the base of the lowest ice lens, which is designated $z_l(t)$. This region consists of alternating layers of ice lenses and soil. Water permeation is not possible in this zone owing to the impermeable ice lenses.

In the frozen fringe the temperature varies within the range $T_l \leq T \leq T_f$, and at coordinate $z_f(t)$, which is defined as the freezing front position corresponding to the frost penetration depth, the ice content vanishes.

As experimental investigations show [20, 21, 23, 24], the moisture distribution in the frozen fringe is characterized by the temperature distribution and,

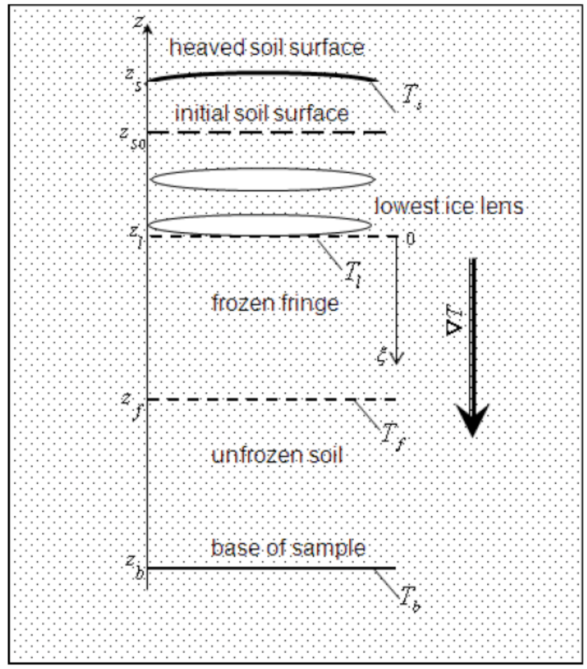

Figure 2: Schematic description of model system: cross-section of soil undergoing a frost heave.

consequently, by the equilibrium water content which is dependent on capillary suction effects and phase transitions. The unfrozen zone is that of ice-free soil $z_b<z<z_f$ which is characterized by a temperature that is higher than the temperature T_f. In the unfrozen zone no freezing is occurring and since the pores are saturated with unfrozen water, we state that $W=\phi$, where $\phi = const$ is soil porosity. It is clear that heat transfer occurs within all zones in the calculation domain.

The boundary value problem for secondary frost heave is based on a nonlinear system of equations. Even the numerical solution of this problem is very complicated. Therefore, for obtaining the solution, we analyze the physical prerequisites and hypothesis for the considered problem, and based on the estimations of the equation's structure we simplify the generalized model.

In the first stage of the analysis we turn to the following dimensionless variables:

$$\left.\begin{array}{l} \bar{z}=\dfrac{z}{H_0} \quad , \quad \bar{t}=\dfrac{t}{t_0} \quad , \quad t_0=\dfrac{H_0}{U_0} , \\ \bar{U}=\dfrac{U}{U_0} \quad , \quad \bar{\mathrm{v}}_s=\dfrac{\mathrm{v}_s}{U_0} \quad , \quad \bar{\mathrm{v}}_i=\dfrac{\mathrm{v}_i}{U_0} \\ \theta=\dfrac{T-T_f}{T_f-T_s} \; , \; \bar{k}=\dfrac{k}{k_{unfr}} \; , \; \bar{S}_{fr}=\dfrac{S_{fr}}{\rho_w U_0 / H_0} \end{array}\right\} , \qquad (2.1)$$

in which $H_0 = z_{s0} - z_b$ is a length scale and z_{s0} is the initial coordinate of the soil surface. We note that in laboratory experiments $z_b = 0$ and z_{s0} are the bottom and top of the sample, respectively, so that H_0 is the height of the sample. Since the frost-penetration depth (freezing front coordinate) z_f occurs between coordinates z_b and z_{s0}, the value H_0 is also a representative length scale for the conduction process. For the freezing front propagation velocity $V_f = dz_f/dt$, ice velocity v_i and, consequently, for the frost heave rate $\mathrm{v}_s = dz_s/dt$ we define the velocity scale U_0, which also characterizes the time scale t_0. As a scale for both the capillary suction and the other pressure variables we take σ which is the characteristic value of the cryostatic suction; for example $\bar{f} = f/\sigma$, $\bar{p}_w = p_w/\sigma$ etc.

Using these variables and for convenience dropping in following the line over values with the understanding that the appropriate values have dimensionless form, the process can be described by boundary value problem in the dimensionless form:

within the frozen zone, where $z_l < z < z_s$

$$Pe\frac{d\theta}{dt} = \nabla \cdot \left(\bar{k}\nabla\theta\right); \tag{2.2}$$

within the frozen fringe, where $z_f < z < z_l$

$$Pe\frac{d\theta}{dt} = \nabla \cdot \left(\bar{k}\nabla\theta\right) + \frac{Pe}{Ste}S_{fr}, \tag{2.3}$$

$$W_t + \nabla \cdot \mathbf{U} = -S_{fr}, \tag{2.4}$$

$$I_t + \nabla \cdot \mathbf{V} = \frac{1}{1-\delta}S_{fr}, \tag{2.5}$$

$$W + I = \phi. \tag{2.6}$$

Within the unfrozen zone the pores of the soil are saturated with water, i.e. $W = \phi$, and the energy equation is given by following equation:

$$z_b < z < z_f \qquad Pe\frac{d\theta}{dt} = \nabla^2\theta. \tag{2.7}$$

In the equations (2. 2), (2.3) and (2.7) *d/dt* = ∂/∂*t* + **U**·∇ is the substantial (total) derivative. The Stefan and Peclet numbers are defined as follows:

$$Ste = \frac{C_p(T_f - T_s)}{\rho_w L}, \quad Pe = \frac{U_0 H_0}{\alpha}, \tag{2.8}$$

where α is thermal diffusivity.

In Eqs. (2.3)-(2.6) W_t and I_t denote the derivatives of water and ice volume fractions with respect to time, respectively; $\mathbf{U}$ and $\mathbf{V}$ are the water and ice fluxes; S_{fr} is the freezing rate; $\delta = 1 - \rho_i/\rho_w$ characterizes the ratio of the ice and water densities. The ice flux $\mathbf{V}$ in Eq. (2.5) is given by

$$\mathbf{V} = I\,\mathbf{v}_i, \tag{2.9}$$

where $\mathbf{v}_i$ is the ice velocity.

Now we assume that the water permeation flux in dimensionless variables is given by Darcy's law in following form:

$$\mathbf{U} = -\frac{k_h\sigma}{\rho_w g H_0 U_0}\nabla p_w, \tag{2.10}$$

in which g is gravitational acceleration and k_h is hydraulic conductivity defined as

$$k_h = k_0\left(\frac{W}{\phi}\right)^{\gamma}, \tag{2.11}$$

where k_0 and γ are constants characteristic of the appropriate soil type. In particular, the constant k_0 is $k_0 = 10^{-12} \div 10^{-10}\, m/s$ for clay, $k_0 = 10^{-9} \div 10^{-7}\, m/s$ for silt and $k_0 = 10^{-4} \div 10^{-2}\, m/s$ for sand [30].

Hydraulic conductivity is an essential characteristic of water migration in porous media under conditions of Darcy's law. In our study in order to obtain an analytical solution we use the power function of saturation $S = W/\phi$ in the form of Eq. (2.11). This function satisfactorily describes the hydraulic conductivity as a function of saturation. For the verification of equation (2.11) we compare (Figure **3**) the calculated results of the hydraulic conductivity k_h for silt loam soil obtained on the basis of the present model ($\phi = 0{,}481$, $k_0 = 10^{-7}\, m/s$) – Eq. (2.11) and model (Eq. (15), Figure **8**) in the work of Watanabe and Flury [38]. It can be seen in Figure **3** that the results of the two calculations are in a good agreement.

It should be noted that in study of O'Neill and Miller [27] it was assumed that soil particles are held

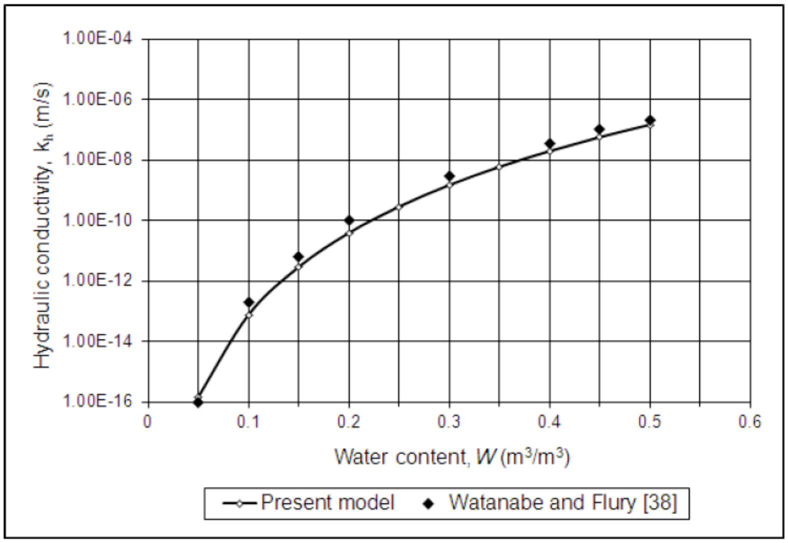

Figure 3: Hydraulic conductivity for the silt loam soil: comparison between calculation results obtained on the basis of the present model ($\phi = 0{,}481$, $k_0 = 10^{-7}\ m/s$) – Eq. (2.11) and model of Eq. (15) – Figure **8** in study of Watanabe and Flury [38].

stationary and thermal regelation will cause ice in the frozen fringe to move towards the ice lens. The lens and pore ice in this model are continuously connected – "*rigid ice model*", and the rate of heaved soil surface – rate of the frost heave is defined by ice velocity:

$$\mathbf{v}_s = \mathbf{v}_i(t). \tag{2.12}$$

As was mention in introduction, Fowler & Krantz [30] suggest that, in general, the ice velocity established by Gilpin [28]. In accordance with Gilpin's concept, the condition for frost heave rate can be written as

$$\mathbf{v}_i - \mathbf{v}_s = -\lambda \nabla T, \tag{2.13}$$

where λ is an empirical constant.

Although these two models for *thermal regelation* give different result, for the solution we use both models. Moreover, in analysis we estimated and give the conditions for the use of each model.

2.2. Initial, Boundary and Supplementary Conditions. Criterion of the Ice Lenses Formation

According to the problem, the initial and boundary conditions can be written as follows. Since we consider the porous media to be saturated, in general, the initial conditions for the temperature and moisture can be described as

$$t = 0 \quad T = T_0, \quad W = W_0 \tag{2.14}$$

The boundary conditions are defined by the equation using the appropriate physical value, as well as by the state of the system undergoing the freezing process. For the freezing process at time $t > 0$, at the top boundary of the system (heaved soil surface) $z_s(t)$ and at the bottom boundary of the calculated domain z_b, we set the appropriate constant temperatures T_s, which are lower than the initial phase-transition temperature, and $T_b = T_0 > T_f$. Also at the boundary $z = z_b$ the pressure $p_w = p_\infty$ must be specified. At the boundary z_f we assume the continuity of the temperature and water pressure, and also water permeation flux. At the most recently formed ice lens boundary z_l we assume the continuity of the temperature. In this case the temperature at this boundary is found in the course of finding the solution (as was mentioned in the introduction, we do not use the Clapeyron relation for the temperature distribution in the frozen fringe). The pressure at the base of the lowest ice lens p_i is equal to the load (overburden) pressure P.

It is necessary to note that since the pressures p_i and p_w are related *via* the cryostatic suction for given type soil as following

$$p_i - p_w = f(W), \tag{2.15}$$

the boundary condition at the base of the lowest ice lens is equivalent to the boundary condition for the unfrozen water pressure:

$$p_{wl} = P - f(W_l) \tag{2.16}$$

In the last equation the index (subscript) 'l' indicates a value, the quantity of which is found at the boundary $z = z_l$. The capillary relation function $f(W)$ for different soils is experimentally measured (see for example [26]) and is represented in Figure **4A** in terms of soil saturation $S = W/\phi$ or as function of moisture W (Figure **4B**). The character of the curves is related to the soil type. For all types of soil the function $f(\phi) = 0$.

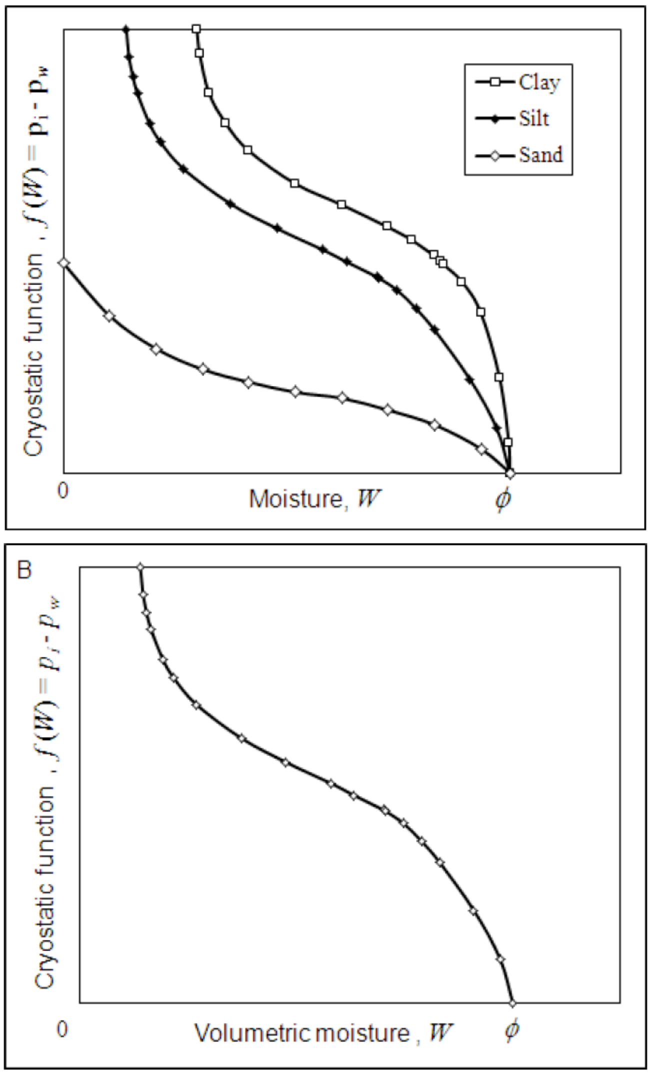

Figure 4: Schematic description of cryostatic suction function: **A** – dependence on saturation for different types of soil; **B** – as a function of volumetric moisture for specific soil.

As a supplementary relation, we consider the total pressure balance in the form [30]:

$$P = p_e + (1-\chi)p_i + \chi p_w, \tag{2.17}$$

in which P and p_e are the overburden pressure and the effective stress exerted by the soil grains when they are in contact, respectively; $\chi(W)$ is the stress partition function which can be represented as

$$\chi = \left(\frac{W}{\phi}\right)^r, \tag{2.18}$$

where r is an empirical constant.

The relationship (2.17) may be written more conveniently as

$$P = p_e + p_w + (1-\chi)(p_i - p_w) \tag{2.19}$$

or in the following form:

$$P = p_e + p_w + (1-\chi)f(W). \tag{2.20}$$

Since in the course of ice lens formation soil particles will readily separate, in this case the effective stress $p_e = 0$. This fact can be considered as a criterion, and therefore from the Eq. (2.20) we obtain, after a simple transformation, the mathematical description of the criterion for initiating a new ice lens as

$$P - p_w = [1-\chi(W)]f(W) \tag{2.21}$$

In Figure **5** we present a graph of the left- and right-hand sides of the equation (2.21) in the form $p_w - P$ and $-(1-\chi)f(W)$, respectively, as a function of ξ – a coordinate measured as the positive downward distance from the lowest ice lens coordinate z_l (Figure **2**). , The water pressure p_w is obtained by solving equation (2.10).

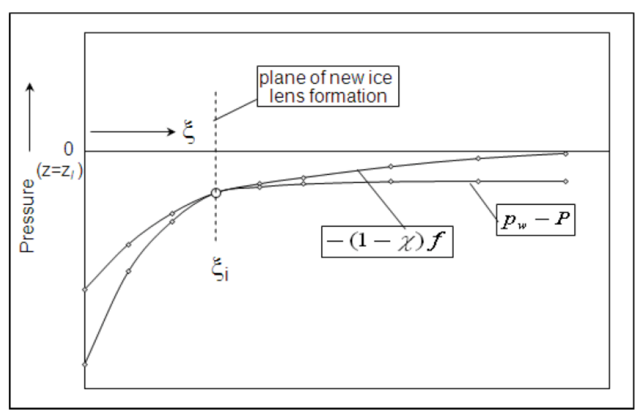

Figure 5: Conditions for ice-lens initiation: distribution of both $-(1-\chi)$ and $p_w - P$ as a function of coordinate ξ.

Both quantities are monotonic and increasing with increasing ξ and hence lens initiation will occur when these curves have a tangency. From Figure **5** it can be seen that the point of tangency for these curves occurs within the water pressure boundary layer and the shape of $p_w - P$ arises from the value $-f_l = -f(W_l)$ at

$\xi = 0$ to the asymptotic value $p_\infty - P$ as $\xi \to \infty$. The character of the water pressure distribution shows that within the permeation boundary layer $p_w \approx p_\infty$. In this case according to the solution of the equation (2.21) the value of the moisture, corresponding to pressure $p_l \equiv p_{wl}$ at the boundary of lowest ice lens, is $W \approx W_l$. Hence, the criterion for new ice lens formation can be written as follows:

$$P - p_\infty = (1 - \chi_l) f_l \,, \tag{2.22}$$

where $\chi_l = \chi(W_l)$ and $f_l = f(W_l)$.

For the determination of the frost heave rate and freezing front velocity, we reduce the frozen fringe to a moving planar boundary, across of which jump boundary conditions are prescribed. These conditions can be obtained by the integration of the mass and energy balances across the frozen fringe [39]. The derivation of these relations we will provide in the next section after some simplification and conversion of the boundary value problem for the dimensionless variables.

3. SIMPLIFICATION OF THE MODEL AND SOLUTION

The dimensionless form of the problem allows us to estimate the terms of the equations and to consider appropriate simplifications that will permit the solution of the problem. For this purpose it can be assumed that the length of interval δ_f of the local phase transition is extremely small. The estimation of this interval can be obtained on the base of likeness and dimension analysis arising from the following physical considerations and have been discussed in details in our previous study [33]. Here we note only some results.

In particular, the crystallization process and water migration within interval δ_f (kinetic zone) should be commensurate. Namely, both effects should be values of the same order of magnitude. If t_* is the characteristic time of the crystallization reaction in the frozen fringe and $\mathbf{U}$ is a permeation flux of unfrozen water migration, then the condition of conformity of these processes can be written as

$$O\left(\frac{\partial I}{\partial t}\right) = O\left(\nabla \cdot \mathbf{U}\right). \tag{3.1}$$

If we set the order of magnitude of each value, taking into consideration Eq. (2.10), we obtain in dimensional variables the following relation:

$$\bar{\delta}_f = \frac{k_0 \sigma}{\rho_w g H_0 U_0} \quad , \tag{3.2}$$

where

$$\bar{\delta}_f = \frac{\delta_f}{H_0}. \tag{3.3}$$

The characteristic values for the parameters into Eq. (3.2) are σ~1 *bar*, $\rho_w = 10^3\, kg/m^3$, $g = 10\, m/s^2$, $k_0 \sim 10^{-11} \div 10^{-12}\, m/s$ (for fine-grained soils), H_0 ~1*m*. The characteristic magnitude of water permeation velocity $U_0 \sim 10^{-8}\, m/s$ is known from experimental investigations [3, 4, 16, 21]. By substituting these values into Eq. (3.2) we see that the dimensionless length of the frozen fringe has changed approximately within interval $10^{-3} \le \bar{\delta}_f \le 10^{-2}$. This estimation implies that the frozen fringe can be assumed to be a free planar boundary.

Since the ice lenses prevent any water migration into zone $z_l < z < z_s$ there is no advection above the frozen fringe. In this case the equation (2. 2) can be rewritten in the simple form:

$$\text{for } z > z_l \qquad \nabla \cdot \left(\bar{k} \nabla \theta\right) = 0\,. \tag{3.4}$$

In the unfrozen zone the Peclet number, characterizing the ratio of the heat advection to heat conduction, can be defined as

$$Pe = \frac{|\mathbf{U}| H_0}{\alpha}. \tag{3.5}$$

As was mentioned above, the water permeation velocity $|\mathbf{U}| = U_0 \sim 10^{-8}\, m/s$, $\alpha \sim 10^{-6}\, m^2/s$, hence the Peclet number $Pe \sim 10^{-2}$, thus implying that sensible heat advection can be ignored, and Eq. (2.7) can be represented in the following form:

$$\text{for } z < z_f \qquad \nabla^2 \theta = 0\,. \tag{3.6}$$

Attention should be paid to the fact that in the freezing of fine-grained soils under natural and experimental temperature gradients, the Stefan number can be changed within a relatively wide range: from 0.0083 to 0.056 [3, 16, 21]. Hence, although the Peclet number can be far less than one, $Pe << 1$ the ratio Pe/Ste is able to take values smaller, equal and larger than one. In this connection, the energy conservation equation (2.3) within the frozen fringe can be represented in the form:

for $z_f < z < z_l \qquad \nabla \cdot \left(\bar{k} \nabla \theta\right) + \frac{Pe}{Ste} S_{fr} = 0$. (3.7)

In order to eliminate the freezing rate S_{fr}, we combine the equations (3.7) and (2.4). After some simple transformations we obtain:

$$W_t + \nabla \cdot \left[\mathbf{U} - \bar{k} \frac{Ste}{Pe} \nabla \theta \right] = 0 . \qquad (3.8)$$

We note that the equation (3.8) is more general than the analogous equation in the work of Fowler and Krantz [30] and in case $Pe/Ste = 1$, both equations are reconciled.

After integration of the equation (3.8) across a thin frozen fringe $\left(z_f, z_l\right)$ we obtained the first equation for the solution:

$$W_l V_f = U_l + \frac{Ste}{Pe} \left(\bar{k} \frac{\partial \theta}{\partial n}\bigg|_l - \frac{\partial \theta}{\partial n}\bigg|_f \right), \qquad (3.9)$$

where $V_f \equiv dz_f / dt$ is velocity of phase front propagation.

We recall that the dimensionless conductivity is defined as $\bar{k} = k / k_{unfr}$ (see (2.1)), and therefore for the unfrozen zone $\bar{k} = 1$.

Although we have ignored the frozen fringe, we preserve in our generalized model the main features of the frozen fringe by means of setting appropriate boundary conditions, corresponding to the problem [33].

In order to obtain the quantity of the heave rate V_s, we consider the water mass balance across z_l (the second equation):

$$\left(1 - \delta\right) V_s = U_l + \left(1 - \delta\right)\left(\phi - W_l\right) \mathrm{v}_i , \qquad (3.10)$$

where v_i is an ice velocity.

We remember that the equations (3.9) and (3.10) are equations in dimensionless form, and the indexes (subscripts) '*l*' and '*f*' indicate a value, the quantity of which is found at the boundary $z = z_l$ and $z = z_f$, respectively.

Obtaining the system of equations (3.9)-(3.10) with associated relations makes it possible to find both the frost heave and freezing front propagation (frost penetration) as a function of time.

As an example we consider a one-dimensional freezing process in region $z_b < z < z_s$, which allows us to illustrate the theoretical concepts, principal features and main regularities of secondary frost heave and also to compare theoretical results with experimental investigations.

In this respect we consider two-zone model: frozen zone, for which $z_f < z < z_s$ and unfrozen zone, where the coordinate z varies within the interval $z_b < z < z_f$.

The basic heat transfer equation for these zones is

$$\frac{\partial^2 \theta}{\partial^2 z} = 0 . \qquad (3.11)$$

It is clear that the solutions of Eq. (3.11) for both zones are linear functions, and with boundary conditions $\theta(z_s) = \theta_s = -1$, $\theta(z_f) = \theta_f = 0$ and $\theta(z_b) = \theta_b$ the temperature gradients at the boundaries $z = z_l$ and $z = z_f$ are given by

$$\frac{\partial \theta}{\partial z}\bigg|_l = -\frac{1}{z_s - z_f} , \qquad (3.12)$$

and

$$\frac{\partial \theta}{\partial z}\bigg|_f = -\frac{\theta_b}{z_f - z_b} . \qquad (3.13)$$

We note that for a given overburden pressure P, the W_l can be obtained directly from equation (2.21) according to the dependence of $f\left(W\right)$ and stress partition function $\chi\left(W\right)$. In this way, the value $f_l = f\left(W_l\right)$ can also be found. The permeation flux U_l at the base of the lowest ice lens $z = z_l$ as a function of the temperature gradient can be found from integration of Eq. (2.10) with employing the Eq. (1.1):

$$U_l = -\tilde{\beta} \frac{\partial \theta}{\partial z}\bigg|_l , \qquad (3.14)$$

where

$$\tilde{\beta} = \beta_l \left[f_l - \left(P - p_\infty\right) \right] \cdot \frac{1 + a_0}{\left(1 - a_0 \theta_l\right)^2} \cdot \frac{W_0 - W_{\min}}{W_l} ,$$

$$\beta_l = \frac{\gamma k_l \sigma L}{g k_{unfr} \left(T_f - T_s\right)} \cdot \frac{Ste}{Pe} . \qquad (3.15)$$

Using the equations (3.12)-(3.14) for the temperature gradients and permeation flux, we can write the system of equations (3.9)-(3.10) for the freezing front propagation coordinate (frost-penetration depth) and frost heave in final form:

$$\frac{dz_f}{dt} = -\frac{A}{z_s - z_f} + \frac{B}{z_f - z_b}, \tag{3.16}$$

$$\frac{dz_s}{dt} = \frac{C}{z_s - z_f}, \tag{3.17}$$

where

$$\left.\begin{aligned} A &= \left(\bar{k}\frac{Ste}{Pe} - \tilde{\beta}\right)\cdot\frac{1}{W_l} \\ B &= \theta_b \frac{Ste}{Pe}\cdot\frac{1}{W_l} \end{aligned}\right\}. \tag{3.18}$$

The value C depends on the model of thermal regelation process:

- for "*Rigid ice model*" of Miller

$$C = \beta_R = \frac{\tilde{\beta}}{(1-\delta)\left[1-(\phi - W_l)\right]}, \tag{3.19}$$

- for "Gilpin's model"

$$C = \beta_G = \frac{\tilde{\beta} + \beta_\lambda (1-\delta)\cdot(\phi - W_l)}{(1-\delta)\left[1-(\phi - W_l)\right]}, \tag{3.20}$$

With dimensionless parameter

$$\beta_\lambda = \frac{\lambda}{\alpha}\cdot\frac{T_f - T_s}{Pe}. \tag{3.21}$$

Thus equations (3.16) and (3.17) are the closed system of equations that allows us to obtain frost-penetration depth (propagation of the freezing front) and frost heave as functions of time. Upon integration, the frost-penetration V_f and heave rate V_s can also be found.

The above system of equations is subject to the following initial conditions for coordinates z_f and z_s:

at $t = 0$, $z_f = z_s = z_{s0}$, (3.22)

where z_{s0} is initial soil surface (**Figure 2**).

The non-linear problem (3.16), (3.17), (3.22) was solved by Runge-Kutta method.

4. RESULTS AND DISCUSSION

The complete analysis of the model for secondary frost heave is described in our previous paper [33]. In

Table 1: Thermal and Physical Properties of Silt-Loamy Soil

Property	Symbol	Value
water density	ρ_w	$10^3\, kg/m^3$
ice density	ρ_i	$0.917\cdot 10^3\, kg/m^3$
thermal conductivity	k	$4.0\, W/(mK)$
heat capacity	C_p	$3.0\cdot 10^6\, J/(kgK)$
soil porosity	ϕ	0.481
initial volumetric moisture	W_0	$0.41\, m^3/m^3$
minimal volumetric moisture	$W_{\min}$	$0.14\, m^3/m^3$
pressure scale	σ	$1.0\, bar$
hydraulic conductivity exponent	γ	9
hydraulic conductivity	k_0	$3.58\cdot 10^{-8}\, m/s$
Gilpin's model constant	λ	$10^{-10}\left(m^2\right)/(sK)$

this section we confine ourselves to some main results. The attention is paid mainly on the evaluation of the model for its ability to predict frost heave and freezing front propagation. In this respect the comparison between calculation results and experimental investigations is analyzed. In particular, for the verification of model we compare results of the modeling with experimental study carried out by Konrad [1] and related to the approach for the prediction of segregation potential using frost heave.

In addition, we give the rate of the frost heave V_s and velocity of phase front propagation V_f and also discuss the effect of hydraulic conductivity on the calculated results and as a consequence on the conformity between Miller's and Gilpin's models. The main information on the thermal and physical properties for the silt-loamy soil and additional data required for the modeling are listed in Table **1**. The cryostatic suction function $f(W)$ was calculated by approximation represented in study by Noon [32].

Figure **6** illustrates the freezing front propagation (frost-penetration) velocity and heave rate.

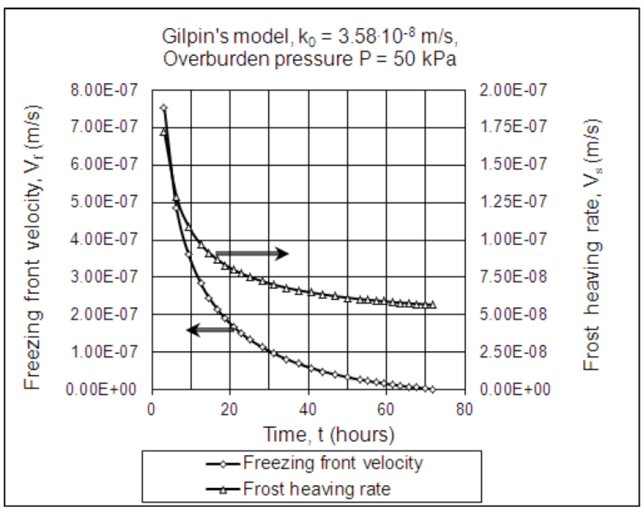

Figure 6: Freezing front velocity and heave rate as a function of time.

As follows from the graph, the heave rate approaches (for the large time) the asymptotic solution $dz_s/dt = V_s(t) = const$, which characterizes the slope of the function $h_s(t) = z_s(t) - z_{s0}$. For this (large) time the function $h_s(t)$ is linear. As was expected, the velocity of the freezing front propagation $V_f(t)$ tends to zero, $\lim_{t\to\infty} V_f(t) = 0$ that corresponds to the stoppage of the freezing front at certain distance from the cold boundary. It should be noted that these characteristics are essential for the prediction of frost heave and its preventing at the level of design and construction.

The next figure compares results obtained under conditions of the different models of the thermal regelation process. In the literature, in particular in the study of Fowler, Krantz (1994 p.1655), it is concluded that "these two models for thermal regelation will yield different result". Indeed, in general the Miller's and Gilpin's models lead to different results (see equations (3.19) and (3.20)). Nevertheless, it is interesting to find under which conditions these two models lead to the same results for frost heave characteristics.

For this purpose the Figure **7A** plots the dependence of the coefficients β_R for rigid ice approximation and β_G for Gilpin's models, respectively, on hydraulic conductivity k_0 which is defined by soil structure and thereby characterizes the type of soil. For convenience the graphs are done in logarithmic coordinates. The hydraulic conductivity coefficient k_0 is varied over a wide range, which characterizes the full spectrum of clayey soils. It can be seen that beginning from the values of $k_0 \approx 2.0\cdot10^{-10}\, m/s$ and higher (for silt and silty-loam soils) the coefficients β_R and β_G are concurrent (4.2A), and both models lead to the same results (Figure **7B**). On the other hand, decreasing the coefficient k_0 leads to different results in the models (Figure **7C**) and the discrepancy between the solutions increases with decreasing values of hydraulic conductivity. These calculation results arise from analysis of the coefficients β_R and β_G, based on equations (3.19) and (3.20). It follows from these equations that in the case when $O(\tilde{\beta}) \gg O(\beta_\lambda \cdot (1-\delta)\cdot(\phi - W_l))$, coefficients $\beta_G \approx \beta_R$ with high accuracy.

As a final result, we present the comparison of the appropriate distributions of frost heave and freezing front propagation (frost depth) calculated using the solution from this model and experimental data obtained by Konrad [1]. As an example, we considered the experiment for the sample of limestone 3, initial material thickness of which was $H_0 = 97\, mm$ and water at the boundary z_l (in our notation), measured after freezing, was $W_l = 21\%$, respectively. The temperatures at the cold and warm boundaries were held constant $-4.1°C$ and $1.5°C$, respectively.

We note that the thermal properties of the limestone and other information for our solution are absent in the

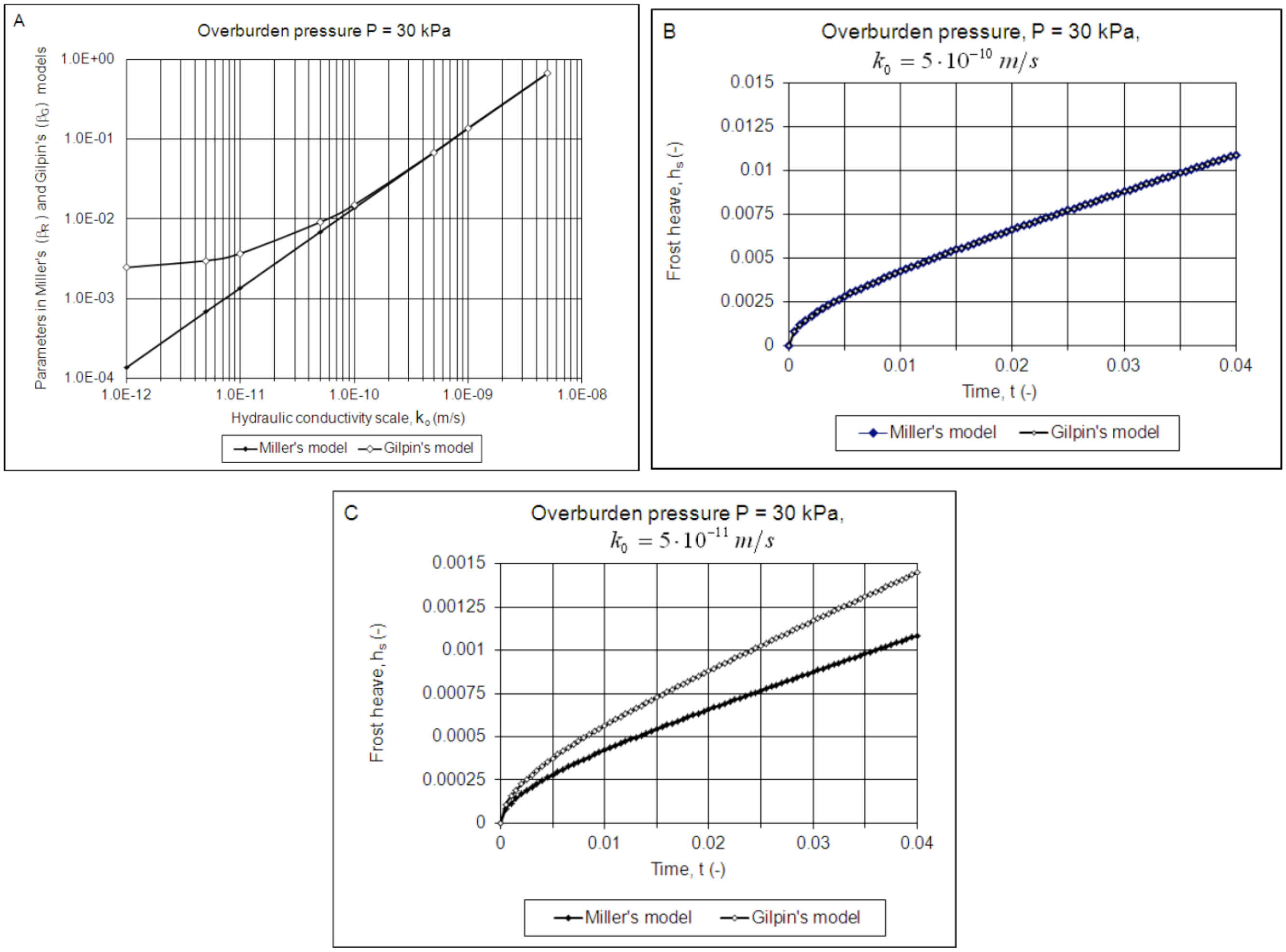

Figure 7: Comparison between Gilpin's and Miller's models: **A** – dimensionless coefficients of Miller's (β_R) and Gilpin's (β_G) models depending on hydraulic conductivity scale k_0 (soil types); **B** – frost heave evolution for $k_0 = 5 \cdot 10^{-10}\ m/s$; **C** – frost heave evolution for $k_0 = 5 \cdot 10^{-11}\ m/s$.

cited work. Therefore, characteristics for frozen and unfrozen zones, conforming to given experimental values of skeleton density and moisture, were borrowed from the book of Feldman ([2], p. 26). Figure **8** illustrates the comparison of the experimental results for the frost heave distribution (Figure **8A**) and also for freezing front propagation – frost depth (Figure **8B**) in the sample, subjected to an overburden pressure of 20 kPa, with calculations obtained by application of the present model.

It is shown that the calculated frost heave and frost depth curves match the experimental results very closely. The discrepancy does not exceed 3.0% for the frost heave and 5.5% for the frost depth (see error bar on the graphs). The results of comparison indicate that the model presented can satisfactorily reproduce the frost heaving process associated with freezing and can be used as predictor for studied phenomenon at the design stages.

5. A MODEL OF ICE LENSES FORMATION

The ice lenses formation in freezing porous media is interesting but at the same time is very complicated problem. As was mentioned in introduction the theoretical and experimental studies on frost heave phenomenon and ice lenses formation goes back to the 1920s and up to recent time [1, 7, 8, 27, 28, 30, 32, 40-42].

For example Taber [7] established that the pressure from frost heaving is due to the direction of ice crystal growth, which is, in turn, controlled by the direction of heat loss. He also observed [8] that the rate of heave is continuous under constant temperatures applied at the top and bottom of soil specimens even though the ice

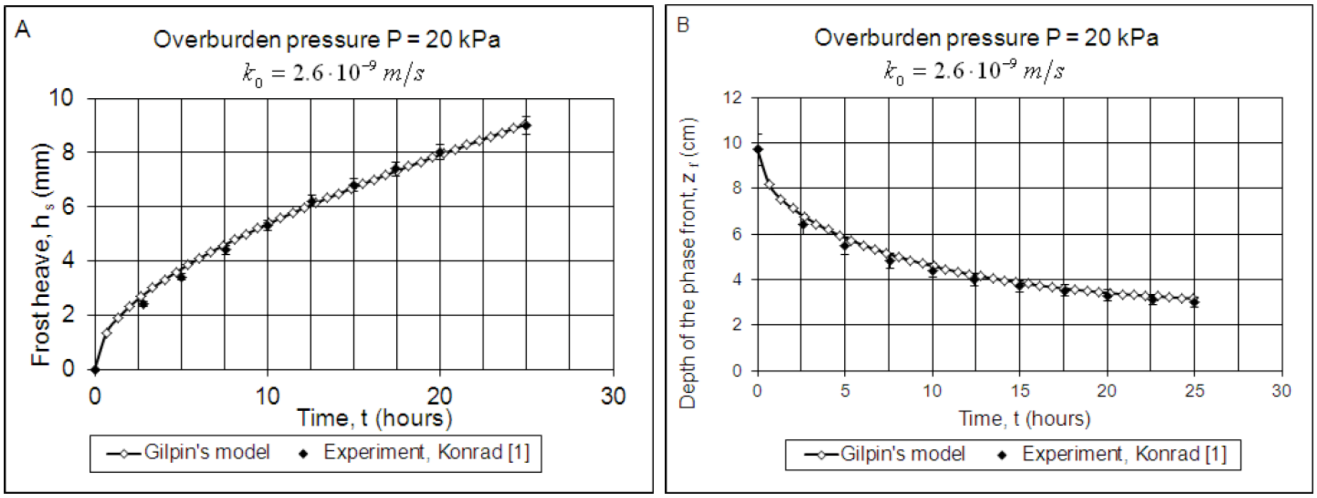

Figure 8: Comparison of modeling with experimental results (Konrad, 2005) for overburden pressure of $20\,kPa$: **A** – frost heave, **B** – frost depth (freezing front propagation).

lenses are separate and distinct from each other. Moreover, the experimental investigations show that the displacement of ice lenses is normal to the phase front propagation; spacing and thickness of ice lenses are increased due time (Figure **9A**). The same results were obtained by Watanabe and Mizoguchi [42] seventy years later (Figure **9B**).

It should be noted that there is sufficiently wide spectrum of mathematical models in scientific literature on the freezing in porous media. Nevertheless, there is not common approach to the considered problem.

In present study, on the basis of physical process we try to develop of the mathematical model for calculation of the very important parameters of ice lenses formation – distance (spacing) $D_l = z_l - z_i$ between lenses and their thickness h_l as functions of time (see Figure **5**). In this connection we consider the criterion (Eq. (2.21)) of ice lens formation:

$$P - p_w = [1 - \chi(W)] f(W)\,. \qquad (5.1)$$

The capillary pressure can be obtained from Darcy's law (2.10), which for 1D problem has a form:

$$U = -\frac{k_h \sigma}{\rho_w g H_0 U_0} \cdot \frac{\partial p_w}{\partial z}\,.$$

Taken into account the relation of derivatives $\partial p_w / \partial \xi = -\partial p_w / \partial z$ (see Figure **2**), the last equation can be rewritten as

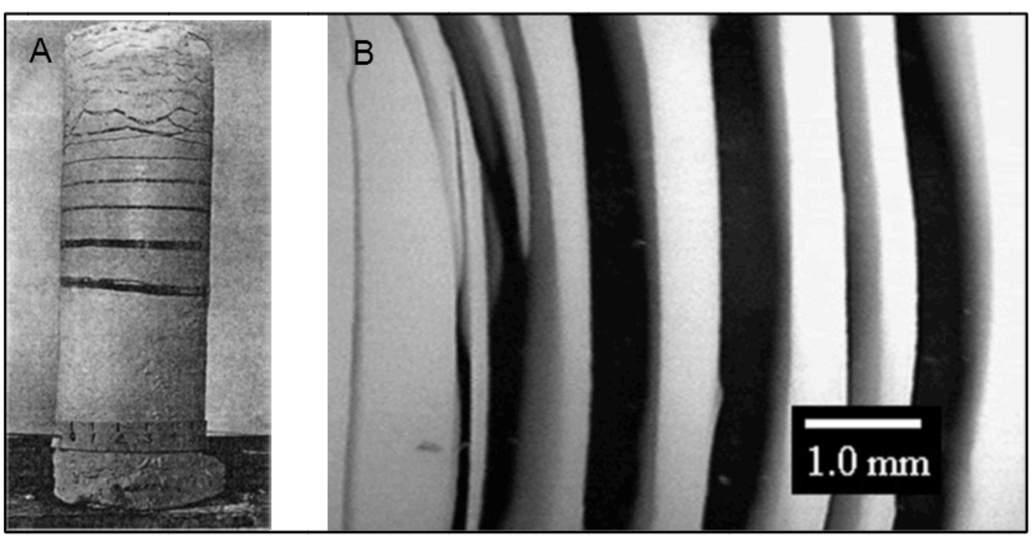

Figure 9: Ice lenses formation (the ice lenses appear black): **A** – experiment by Taber [8]; freezing from top of soil specimen. **B** – experiment by Watanabe and Mizoguchi [42] (right-hand side is colder).

$$U_\xi = \frac{k_h \sigma}{\rho_w g H_0 U_0} \cdot \frac{\partial p_w}{\partial \xi} \quad , \tag{5.2}$$

where the hydraulic conductivity k_h is defined by Eq. (2.11).

By expansion of the function $W(\xi)$ in Taylor series in vicinity of the point $\xi = 0$ that corresponds to point $z = z_l$ (Figures **2** and **5**) we obtain that

$$U_\xi = \frac{k_0 \sigma}{\rho_w g H_0 U_0} \cdot \frac{1}{\phi^\gamma} \left(W_l + W_l' \xi \right)^\gamma \frac{\partial p_w}{\partial \xi}$$

or in other form:

$$U_\xi = \frac{k_l \sigma}{\rho_w g H_0 U_0} \left(1 + \frac{W_l'}{W_l} \xi \right)^\gamma \cdot \frac{\partial p_w}{\partial \xi}, \tag{5.3}$$

where

$$k_l = k_0 \left(\frac{W_l}{\phi} \right)^\gamma . \tag{5.4}$$

According to the properties of the logarithmic function we can rewrite the last equation in following form:

$$U_\xi = \frac{k_l \sigma}{\rho_w g H_0 U_0} exp \left(ln \left(1 + \frac{W_l'}{W_l} \xi \right)^\gamma \right) \cdot \frac{\partial p_w}{\partial \xi}. \tag{5.5}$$

By expansion of the logarithmic function in Taylor series in vicinity of the point $\xi = 0$ the equation (5.5) can be written as

$$U_\xi = \frac{k_l \sigma}{\rho_w g H_0 U_0} exp \left[\left(\frac{\gamma W_l'}{W_l} \right) \xi \right] \frac{\partial p_w}{\partial \xi} \tag{5.6}$$

Now we represent the Eq. (5.6) in the form of differential equation in respect to capillary pressure p_w

$$\frac{\partial p_w}{\partial \xi} = \frac{\rho_w g H_0 U_0}{k_l \sigma} \cdot U_\xi exp \left(-\frac{\gamma W_l'}{W_l} \xi \right). \tag{5.7}$$

Since U_ξ varies over the length scale of the frozen fringe, whereas the water pressure varies over the permeation boundary layer thickness ($\xi << 1$), and $\gamma = 7 \div 9 >> 1$, the equation (5.7) can be integrated assuming U_ξ to be constant. Using the boundary condition $\lim_{\xi \to \infty} p_w(\xi) = p_\infty$, we obtain the water-pressure profile as

$$p_w = p_\infty - \frac{\rho_w g H_0 U_0}{\gamma k_l \sigma} U_l \frac{W_l}{W_l'} exp \left[-\left(\frac{\gamma W_l'}{W_l} \right) \xi \right]. \tag{5.8}$$

Using the condition $p_i = P$ at the boundary $\xi = 0$ that corresponds to $z = z_l$ (lowest ice lens), in the form of Eq. (2.24), the solution (5.8) gives:

$$P - f(W_l) - p_\infty = -\frac{\rho_w g H_0 U_0}{\gamma k_l \sigma} U_l \frac{W_l}{W_l'}. \tag{5.9}$$

Replacing in Eq. (5.8) the coefficient before exponent by Eq. (5.9) leads to the following function for $p_w(\xi)$

$$p_w(\xi) = p_\infty + \left(P - f(W_l) - p_\infty \right) exp \left[-\left(\frac{\gamma W_l'}{W_l} \right) \xi \right]. \tag{5.10}$$

By substituting solution (5.10) into criterion (5.1) and taken into consideration relation between derivatives $W_l' = \left(\partial W / \partial \xi \right)\big|_{\xi=0} = -\left(\partial W / \partial z \right)\big|_{z=z_l}$ ($\xi = z_l - z$), by invers of the exponent, we obtain:

$$z_l - z = \frac{1}{\gamma} \cdot \frac{W_l}{W_l'} \cdot ln \left(\frac{P - p_\infty - \left[1 - \chi(W) \right] \cdot f(W)}{P - f(W_l) - p_\infty} \right). \tag{5.11}$$

In order to obtain distance between lenses we consider the last equation at the boundary $z = z_i$ of the new lens formation (Figure **5**). This leads to the following solution:

$$D_l = z_l - z_i = \frac{1}{\gamma} \cdot \frac{W_l}{W_l'} \cdot ln \left(\frac{P - p_\infty - \left[1 - \chi(W_i) \right] \cdot f(W_i)}{P - f(W_l) - p_\infty} \right) \tag{5.12}$$

In general it is possible to obtain the second equation relatively to z_i and W_i by equality of the slopes (derivatives) of the left and right functions in Eq. (2.21) (Figure **5**). Nevertheless, assuming that $z_l - z_i$ is small [42] it can be set $W_i \approx W_l$ and spacing between lenses can be calculated by following expression:

$$D_l = z_l - z_i = \frac{1}{\gamma} \cdot \frac{W_l}{W_l'} \cdot ln \left(\frac{P - p_\infty - \left[1 - \chi(W_l) \right] \cdot f(W_l)}{P - f(W_l) - p_\infty} \right). \tag{5.13}$$

The thickness of the lenses can be obtained simply from the physical interpretation of the phase front

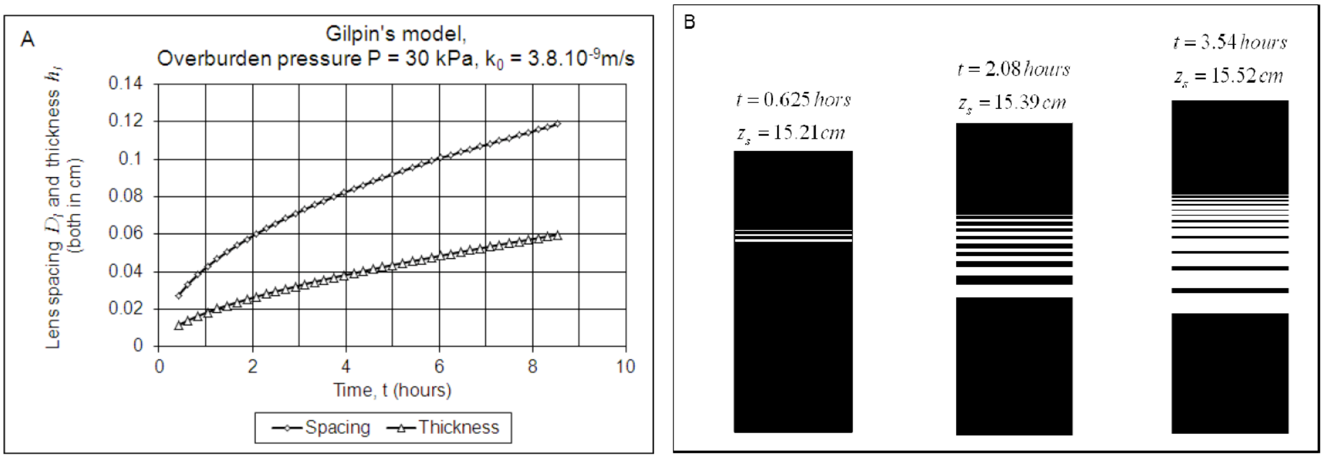

Figure 10: Ice lenses formation in freezing soil: **A** – lenses spacing and lenses thickness against time; **B** – histogram of ice lenses formation at different times.

velocity V_f, heave rate V_s and thermal regelation process.

Let t_l^{n-1} be the time of the formation of the ($n-1$)-th lens. Then t_l^n is given approximately by

$$z_l\left(t_l^{n-1}\right)-z_i\left(t_l^n\right)=D_l\left(t_n^l\right) \tag{5.14}$$

According to *frost heave* and *thermal regelation* processes the thickness of the lens h_l can be defined as

$$h_l=z_s\left(t_l^n\right)-z_s\left(t_l^{n-1}\right)=\Delta t\cdot V_s\,. \tag{5.15}$$

In last equation

$$\Delta t=t_l^n-t_l^{n-1}=\frac{D_l}{V_f}\,. \tag{5.16}$$

By substitution Δt into Eq. (5.15) we obtain relatively simple model of the lens thickness, which is in agreement with experimental results:

$$h_l=D_l\cdot\frac{V_s}{V_f}\,. \tag{5.17}$$

In the equations (5.15)-(5.17) $V_s=dz_s/dt$ and $V_f=dz_f/dt$ are rate of the frost heave and frost penetration velocity.

As an example and verification of the model we give the calculation of the spacing and thickness of the lenses in freezing soil. This calculation was carried out on the basis of following main data: high of sample – $H_0=15\,cm$; overburden pressure $-P=30\,kPa$; hydraulic conductivity $-k_0=3.8\cdot10^{-9}\,m/s$; cooling temperature at the top of sample ($z=z_s$) $-T_s=-1.8°C$; temperature at the bottom of sample ($z=z_b$) – $T_b=1.9°C$. In calculation it was considered Gilpin's model of thermal regelation as a general model (see Introduction and also Section 2). In Figure **10** we plot the lens spacing (distance) and thickness against time (Figure **10A**) and dynamics of the lenses formation in histogram form obtained in present study (Figure **10B**). In the histogram we also give the values of the heaving surface coordinate z_s.

From distributions it can be seen that both characteristics are increasing function of time that is in agreement with experimental investigations (see for example [8, 15, 42], etc.). It is also shown that the absolute values of the lenses' parameters are small. From graphs it can be found that the spacing and thickness of lenses formation after 8 hours exceed $1.2\,mm$ and $0.6\,mm$, respectively.

6. CONCLUSIONS

1. The generalized model for secondary frost heave is presented. In contrast to the models of other authors (in particular, Fowler & Krantz [30]) we recognize the need to determine the distribution of the moisture within the frozen fringe by approximation of experimental data. The equilibrium unfrozen water content reflects the complicated interactions between water, ice and mineral skeleton during the freezing process. The generalization of the Clapeyron relation, which is used in the work cited above, estimates just the drop in initial freezing temperature and does not give a connection with external

temperature gradient which is responsible for the frost heave process.

2. For the determination of freezing front propagation and frost heave, a system of differential equations has been derived and solved by the Runge-Kutta method.

3. It is very important that the system of equations and as a consequence, solution has been obtained in the form of characteristic criteria Peclet (Pe) and Stefan (Ste). This approach allows obtaining the more general solution as well as to analyze the frost heave and propagation of the freezing front as dependent on the convective and phase transition components of the problem.

4. The analysis and comparison of results obtained under conditions of the different models of thermal regelation process – "*Rigid ice approximation*" of Miller and "*Gilpin's model*" are presented. For the first time it is obtained the conditions (criterion) for the use of each model.

5. The criterion of the ice lenses formation in fine-grained soils and the model for calculation of the lenses' thickness and spacing are derived. The histogram of the lenses formation is presented and discussed.

6. The theoretical concepts and the results obtained from the solution presented are in agreement with appropriate experimental investigations. The utilization of this solution for the prediction of the frost heave phenomenon and ice lenses formation in the soil freezing processes shows that the calculated frost heave and other components (frost penetration, heave rate and front velocity) match the experimental results very closely and indicates that the model can well reproduce the frost heaving process.

REFERENCES

[1] Konrad JM. Estimation of the segregation potential of fine-grained soils using the frost heave response of two reference soils. Can Geotechnol J 2005; 42: 38-50. http://dx.doi.org/10.1139/t04-080

[2] Feldman GM. Reference book for the forecast of the soils temperature behaviour. Ac. Sci. of USSR Publisher; Yakutsk 1988.

[3] Ershov ED. The moisture transfer and cryogenic textures in dispersive rocks. Nauka; Moscow 1979.

[4] Danielian YuS. Yanitcky PA. Cheverev VG, Lebedenko YuP. Experimental and theoretical heat and mass transfer research in frozen soils. J Eng Geol 1983; 3: 77-83.

[5] Nakano Y. Mathematical model on the steady growth of an ice layer in freezing soils. in: Maeno N, Mondoh T, Eds. Physics and Chemistry of ice. Hokkaido University Press 1992; pp. 364-369.

[6] Bronfenbrener L, Korin E. Kinetic model for crystallization in porous media. Int J Heat Mass transfer 1997; 40: 1053-59. http://dx.doi.org/10.1016/0017-9310(96)00170-6

[7] Taber S. Frost heaving. J Geol 1929; 37: 428-61. http://dx.doi.org/10.1086/623637

[8] Taber S. The mechanics of frost heaving. J Geol 1930; 38(4): 303-17. http://dx.doi.org/10.1086/623720

[9] Beskow G. Soil freezing and frost heaving with special application to roads and railroads. Swed Geol Soc 1935; Ser. C, No. 375: 26th year book No. 3 (translated by J.O. Osterberg, Northwestern Univ. 1947).

[10] Penner E. The mechanism of frost heave in soils. Highway Res Board Bull 1959; 22: 1-22.

[11] Everett DH. The thermodynamics of frost damage to porous solid. Trans Faraday Soc 1961; 57: 1541-51. http://dx.doi.org/10.1039/tf9615701541

[12] Ershov ED, Williams PJ, Eds. General Geocryology (Studies in Polar Research). Cambridge University Press Publisher; Cambridge 2004.

[13] Grechischev SE, Chistotinov LE, Shur Yu L. Cryogenic physic-geological processes and their prediction, Nedra; Moscow 1980.

[14] Konrad JM, Morgenstern NR. Effects of applied pressure on freezing soils. Can Geotechnol J 1980; 17: 473-86. http://dx.doi.org/10.1139/t80-056

[15] Konrad JM, Morgenstern NR. Mechanistic theory of ice lens formation in finer-grained soils. Can Geotechnol J 1982; 19: 494-505. http://dx.doi.org/10.1139/t82-053

[16] Feldman GM. Moisture movement in melted and frozen soils. Nauka; Novosibirsk 1988.

[17] Furukawa Y, Shimada W. 3-dimensional pattern-formation during growth of ice dendrites, its relation to universal law of dendritic growth. J Crystal Growth 1993; 128: 234-49. http://dx.doi.org/10.1016/0022-0248(93)90325-Q

[18] Anderson DM, Tice AR. The unfrozen interfacial phase in frozen water systems. in: Hadar A, Ed. Ecological Studies: Analysis and Synthesis, New York; Springer 1973; Vol. 4: pp. 107-124.

[19] Fukuda M, Kim H, Kim Y. Preliminary results of frost heave experiments using standard test sample provided by TC8. in: Proceedings of the International Symposium on Ground Freezing and Frost Action in Soils, Lulea, Sweden 1997; pp. 25-30.

[20] Michalowski RL, Zhu M. Frost heave modeling using porosity rate function. J Numer Anal Meth Geomech 2006; 30: 703-22. http://dx.doi.org/10.1002/nag.497

[21] Ershov ED. Phase composition in the frozen rocks. Nauka; Moscow 1979.

[22] Michalowski RL. A constitutive model of saturated soils for frost heave simulations. Cold Regions Sci Technol 1993; 22: 47-63. http://dx.doi.org/10.1016/0165-232X(93)90045-A

[23] Bronfenbrener L, Korin E. Experimental studies of water crystallization in porous media. J Chem Eng Proc 2002; 41: 357-63. http://dx.doi.org/10.1016/S0255-2701(01)00156-8

[24] Bittelli M, Flury F, Roth K. Use of dielectric spectroscopy to estimate ice content in frozen porous media. Water Resour Res 2004; 40: 1-11. http://dx.doi.org/10.1029/2003WR002343

[25] Fasano A, Primicerio M. Freezing in porous media: a review of mathematical models. in: Boffi V, Neunzert H, Eds. Applications of Mathematics in Technology. Teubner 1984; pp. 288-311.

[26] O'Neill K. The physics of mathematical frost heave models: a review. Cold Regions Sci Technol 1983; 6: 275-91. http://dx.doi.org/10.1016/0165-232X(83)90048-4

[27] O'Neill K, Miller RD. Exploration of a rigid ice model of frost heave. Water Resour Res 1985; 21: 1-22. http://dx.doi.org/10.1029/WR021i003p00281

[28] Gilpin RR. A model of the "liquid-like" layer between ice and a substrate with applications to wire regelation and particle migration. J Colloid Interface Sci 1979; 68: 235-251. http://dx.doi.org/10.1016/0021-9797(79)90277-7

[29] Worster MG, Wettlaufer JS. The fluid mechanics of premelted liquid films. in: Shyy W, Narayanan R, Eds. Fluid dynamics of interfaces. Cambridge Cambridge University Press 1999; 339-55.

[30] Fowler AC, Krantz WB. A generalized secondary frost heave model. SIAM J Appl Math 1994; 54(6): 1650-1675. http://dx.doi.org/10.1137/S0036139993252554

[31] Fowler AC, Noon CG. A simplified numerical solution of the Miller model of secondary frost heave. Cold Reg Sci Tech 1993; 21(4): 327-36. http://dx.doi.org/10.1016/0165-232X(93)90010-6

[32] Noon CG. Secondary Frost Heave in Freezing Soils. Ph.D. Thesis, Corpus Christi College, Oxford; Hilary Term 1996.

[33] Bronfenbrener L, Bronfenbrener R. Modeling frost heave in freezing soils. J Cold Reg Sci Technol 2010; 61/1: 43-64. http://dx.doi.org/10.1016/j.coldregions.2009.12.007

[34] Takeda K, Nakano Y. Quasi-steady problems in freezing soils: II. Experiment analysis on steady growth of an ice layer. Cold Reg Sci Technol 1990; 18: 225-47. http://dx.doi.org/10.1016/0165-232X(90)90023-P

[35] Hoekstra P. Moisture movement in soil under temperature gradient with the cold side below freezing. Water Resour Rev 1969; 2: 241-50. http://dx.doi.org/10.1029/WR002i002p00241

[36] Bronfenbrener L, Korin E. Two-phase zone formation conditions under freezing of porous media. J Crystal Growth 1999; 198/199: 89-95. http://dx.doi.org/10.1016/S0022-0248(98)01209-3

[37] Bronfenbrener L. Heat and mass transfer in porous media under phase transition conditions: freezing of soils. Chapter in book: Kong Shuo Tian and He-Jing Shu Eds. Progress in porous media research. New York: Nova Science Publishers 2009; pp. 50-103.

[38] Watanabe K, Flury M. Capillary bundle model of hydraulic conductivity for frozen soil. Water Resour Res 2008; 44; W12402. http://dx.doi.org/10.1029/2008WR007012

[39] Bronfenbrener L. Modelling heat and mass transfer in freezing porous media. Nova Science Publishers, Inc.: New York 2012.

[40] O'Neill K. Miller RD. Numerical solutions for a rigid ice model of secondary frost heave. 2nd International Symposium on Ground Freezing. Trondheim 1980; pp. 656-69.

[41] Rempel AW. Formation of ice lenses and frost heave. J Geophys Res 2007; 11: 1-17.

[42] Watanabe K, Mizoguchi M. Ice configuration near a growing ice lens in a freezing porous medium consisting of micro glass particles. J Crystal Growth 2000; 213: 135-140. http://dx.doi.org/10.1016/S0022-0248(00)00353-5

Received on 13-07-2014 Accepted on 09-08-2014 Published on 23-11-2014

DOI: http://dx.doi.org/10.15377/2409-983X.2014.01.01.1